CONF-790644--5

INTERNATIONAL COLLOQUIUM ON IRRADIATION

TESTS FOR REACTOR SAFETY PROGRAMMES

June 25-28, 1979

PETTEN, THE NETHERLANDS

ULTRASONIC DENSITY DETECTOR FOR VESSEL AND REACTOR CORE TWO-PHASE FLOW MEASUREMENTS

A. E. Arave

Idaho National Engineering Laboratory
EG&G Idaho, Inc.
P.O. Box 1625
Idaho Falls, Idaho 83401
United States of America

ULTRASONIC DENSITY DETECTOR FOR VESSEL AND REACTOR CORE TWO-PHASE FLOW MEASUREMENTS

A. E. Arave
Idaho National Engineering Laboratory
EG&G Idaho, Inc.
P.O. Box 1625
Idaho Falls, Idaho 83401

ABSTRACT

A local ultrasonic density (LUD) detector has been developed by EG&G Idaho, Inc., at the Idaho National Engineering Laboratory for the Loss-of-Fluid Test (LOFT) reactor vessel and core two-phase flow density measurements. The principle of operating the sensor is the change in propagation time of a torsional ultrasonic wave in a metal transmission line as a function of the density of the surrounding media. A theoretical physics model is presented which represents the total propagation time as a function of the sensor modulus of elasticity and polar moment of inertia. Changes in propagation times are related to the polar moment of inertia of the sensor and the density of the surrounding media. The difference between the propagation times in air and water is approximately 3 μs depending on the cross-sectional aspect ratio and length of the sensor. The aspect ratio can vary between 3 and 7 depending on design considerations. The thin side of the sensor is oriented into the flow and varies in width from 0.35 to 1.6 mm depending on the mechanical strength required. Separate effects tests and two-phase flow tests have been conducted to characterize the detector. Tests show the detector can perform in a 343°C pressurized water reactor environment and measure the average density of the media surrounding the sensor.

Steady state air-water tests were conducted to evaluate the effects of flow on the sensor. For superficial air-water velocities greater than 3 m/s, the flow effects are significant when a 6.35- x 1.50-mm sensor is used. In steam-water transient blowdown

tests, correlation with a gamma densitometer reference measurement was excellent except during the mist flow conditions near the end of the blowdown. The overall accuracy was better than to within 100 kg/m^3.

NOMENCLATURE

c	=	Ultrasonic velocity of propagation
d	=	Length of propagation path
t	=	Total propagation time ($t_o + \Delta t$)
t_o	=	Propagation time at initial conditions
Δt	=	Change in propagation time from initial conditions due to density and temperature
Δt_T	=	Change in propagation time from initial conditions due to temperature
Ka	=	Determined by aspect ratio bar
J	=	Inertia of bar and surrounding media
G	=	Modulus of elasticity
ρ_g	=	Density of sensor bar
$\Delta\rho$	=	Change in average density of air-water covering the sensor bar surface from initial conditions
ρe	=	Effective density due to the bar inertia loading at initial conditions
T	=	Temperature of bar
T_o	=	Temperature of initial conditions
K_1, K_2, and K_3	=	Empirically derived constants

INTRODUCTION

The local ultrasonic densitometer (LUD) is a unique detector developed for the Loss-of-Fluid Test (LOFT) facility by EG&G Idaho, Inc., at the Idaho National Engineering Laboratory (INEL). The ultrasonic densitometer provides density measurements in steam-water

mixtures in the reactor vessel for water reactor research safety experiments. The development program for the densitometer started ten years ago with the early instrument development for LOFT when it was recognized that stainless steel interfaces at instrument penetrations into pressurized water reactor (PWR) environments and the characteristics of magnetostrictive ultrasonic transducers have the best survivability[1,2,3]. Later when core inlet and outlet density measurements were needed in LOFT, Panametrics Inc., developed the ultrasonic sensor technique further for the core inlet requirements[4]. Application of a torsional ultrasonic wave in the sensor was developed by Panametrics, Inc., and a detector was designed and fabricated by EG&G Idaho, Inc., for installation in LOFT[5,6].

Further development work was then started to improve the performance by making the detector smaller and by minimizing two-phase flow and temperature sensitivity for high velocity applications. This paper defines the latest technology in design parameters and performance accuracy for small local sensors by describing the density sensor, signal processing system, and magnetostrictive transducer and then by providing details of the sensor characteristics, analytical model, and performance in two-phase flow.

ULTRASONIC DENSITOMETER SYSTEM DESCRIPTION

This section describes the local ultrasonic densitometer (LUD) system including the density sensing theory, the ultrasonic signal, the signal processing system, and the magnetostrictive transducer.

The density sensor is a torsional ultrasonic wave transmission line. The torsional wave propagation velocity is a function of the sensor twisting inertia, modulus of elasticity, and sensor material density. Water surrounding the transmission line increases the inertia forces acting on the sensor and decreases the propagation time. Lynworth[4] has given the following analogy. "Visualize the spinning of an oar about its axis, alternately clockwise (cw) and counterclockwise (ccw), by the 'handsducer' method. Now let the oar

be immersed gradually in a nonviscous liquid in a barrel. As the blade enters the liquid, a large increase in inertia is sensed. The more completely the blade is immersed, the more slowly the oar will be spun, for a constant input torque. Once the paddle is fully immersed, deeper immersion makes the circular handle wet, but does not further impede the rotation. The denser the liquid, the greater its inertia, and likewise its resistance to the oar's accelerations."

A bar of stainless steel with an ultrasonic transducer operating in the pulse-echo mode using the preceding principle can then become a density detector as shown in Figure 1. The magnetostrictive transducer generates an extensional wave that propagates in the extensional wave mode to the point of mode conversion to a torsional wave. The torsional wave can then be transmitted to a rectangular density sensitive sensor. The torsional wave reflects as an echo from the end of the sensor and is received by the same transducer that transmitted it. Echos of various amplitudes also occur at each of the changes in the transmission line configuration depending on the acoustical impedance mismatch. Application of this basic configuration to a specific design is shown in Figure 2 with a typical superimposed wave form for air and water.

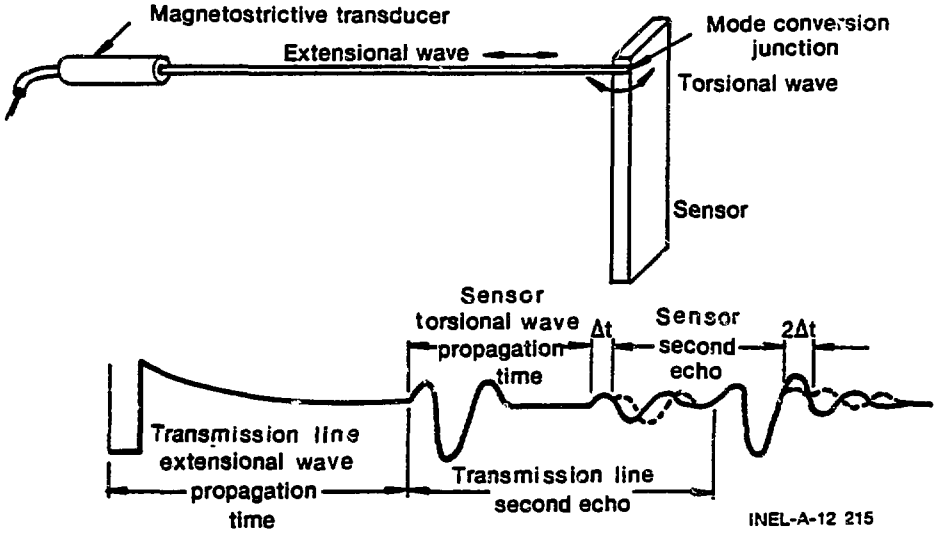

Fig. 1 Basic configuration.

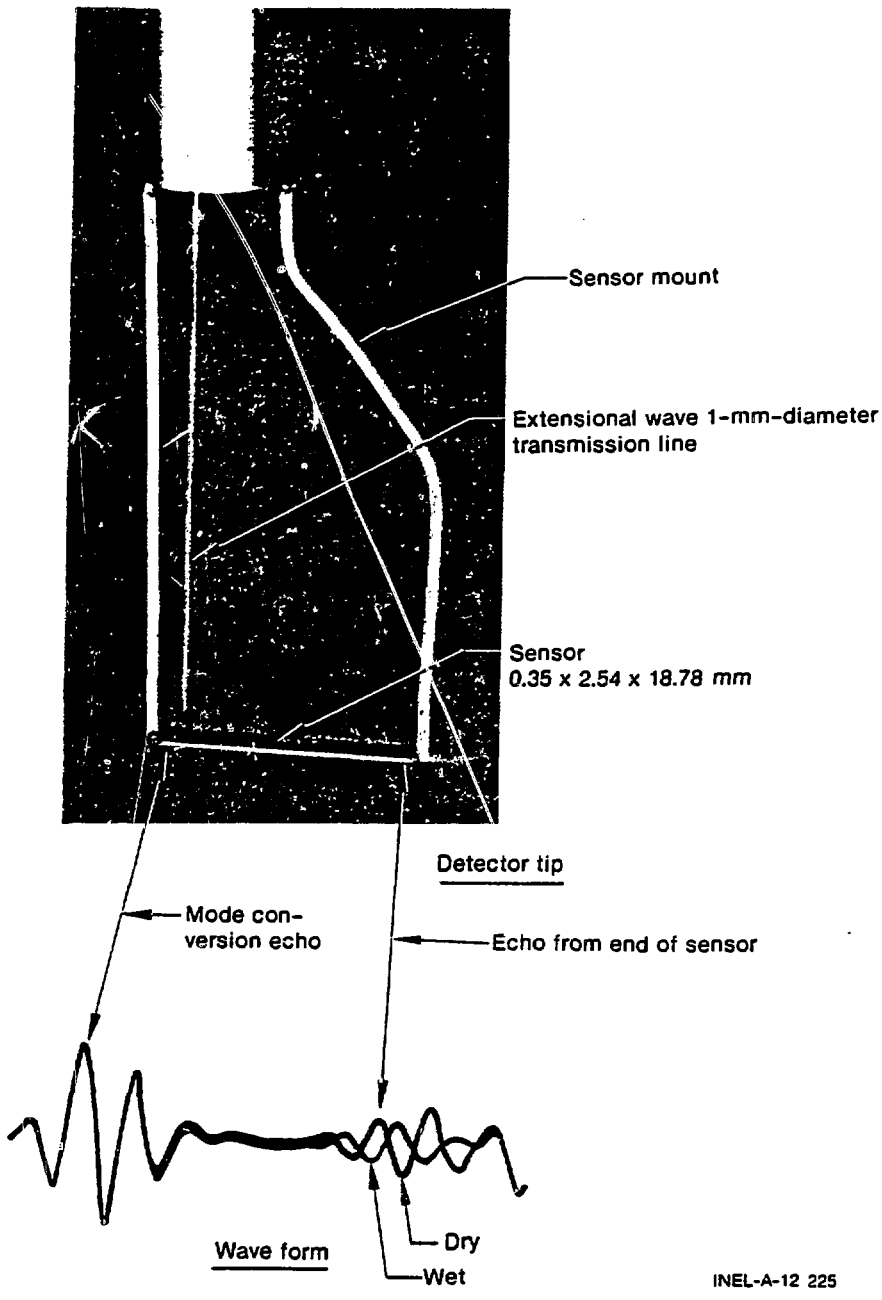

Fig. 2 Possible local ultrasonic density detector configuration.

A block diagram of the LUD signal processing system is shown in Figure 3. The basic operating principle is an accurate time interval measurement. The accuracy is controlled by the 0.01- s electronic resolution for a 1- to 4-μs change in propagation time, depending on sensor length and aspect ratio, and full scale air-water propagation time change from air to water. The 166-kHz ultrasonic-received signal packet is processed through a 100- to 200-kHz band pass filter. Changes in propagation time are measured between the mode conversion extensional wave echo from the one end of the sensor and the torsional wave echo from the opposite end of the sensor as illustrated in Figures 1 and 2. Blanking and amplitude discrimination logic are used to allow the zero crossing detector to provide a pulse for the predetermined zero crossing reference echos desired. The air-water density sensitivity is less than one period for ease in zero crossing tracking. An analog output proportional to the length of the time interval measured is provided.

The technology for the magnetostrictive ultrasonic transducer is the same as that for inpile ultrasonic fuel centerline thermometry[7,8]. A typical magnetostrictive transducer is shown in Figure 4. The transducer is capable of surviving at temperatures between 650 and 900°C depending on the ceramic insulation, electrical conductor material, and splicing technique used. All materials are capable of surviving in a nuclear environment of $>10^{18}$ nvt. A typical transducer provides a carrier frequency of about 166 kHz when a 1-mm-diameter, 13-mm-long Remendur[a] magnetostrictive stub is used. The coil is also 13 mm long and is contained in a 5-mm-diameter, 25-mm-long stainless steel housing.

---

a. Remendur is a trade name for a magnetostrictive material made of 49% cobalt, 49% iron, and 2% vanadium.

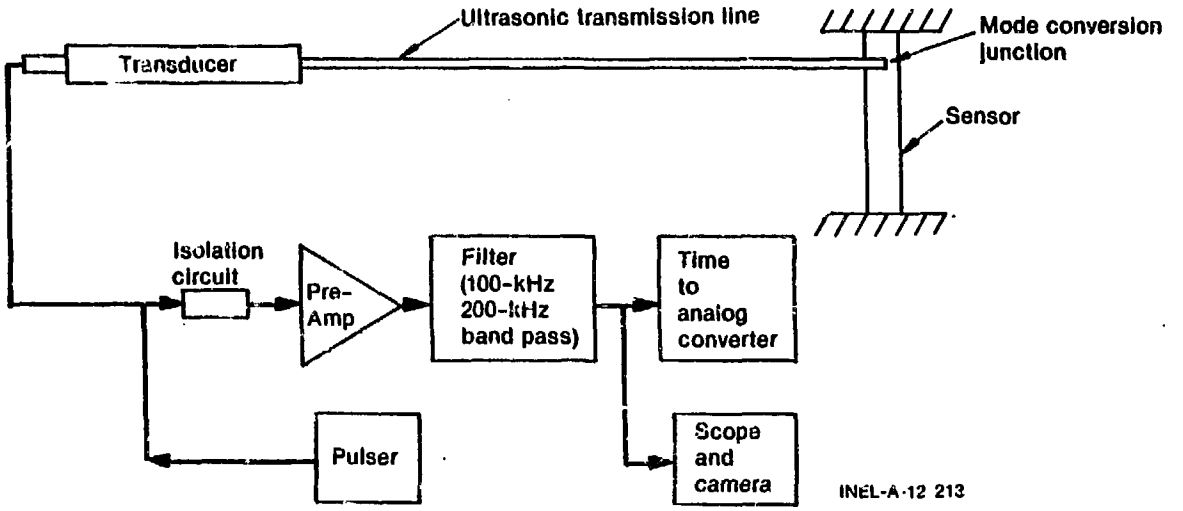

Fig. 3 Local ultrasonic density detector system.

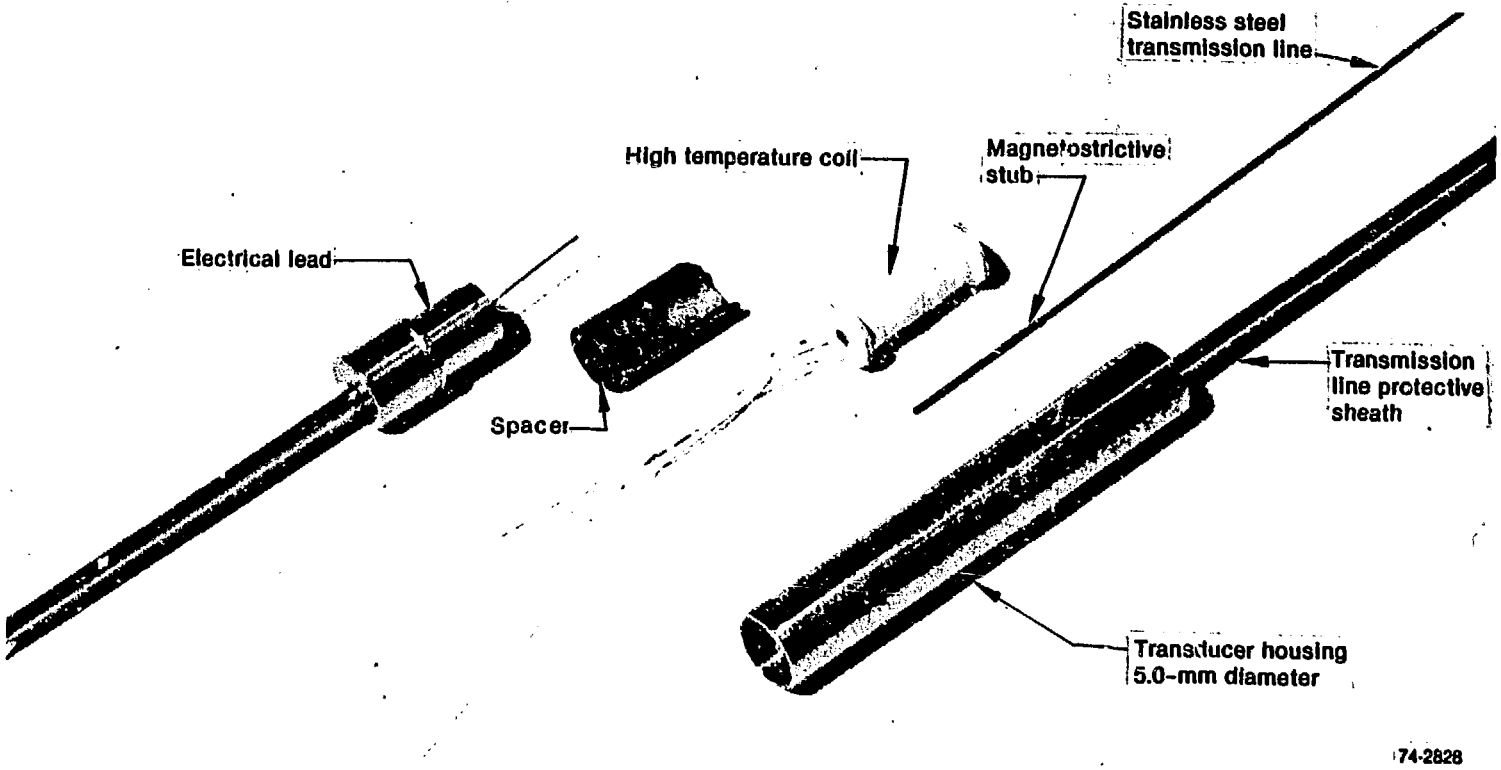

Fig. 4 A typical magnetostrictive, ultrasonic transducer.

SENSOR CHARACTERISTICS VERSUS SHAPE

The sensitivity of the sensor to single-phase fluid density in terms of torsional wave propagation time was shown to be directly proportional and a function of sensor width to the thickness aspect ratio by Lynworth[4] in his investigations as shown in Figure 5. The polar moment of inertia is proportional to the width of the thickness aspect ratio. The propagation velocity as a function of the aspect ratio and the polar moment of inertia for rectangular, wedge, and oval-shaped sensors was checked for design purposes and is listed in Table I. The percentage of air-to-water propagation time changes was

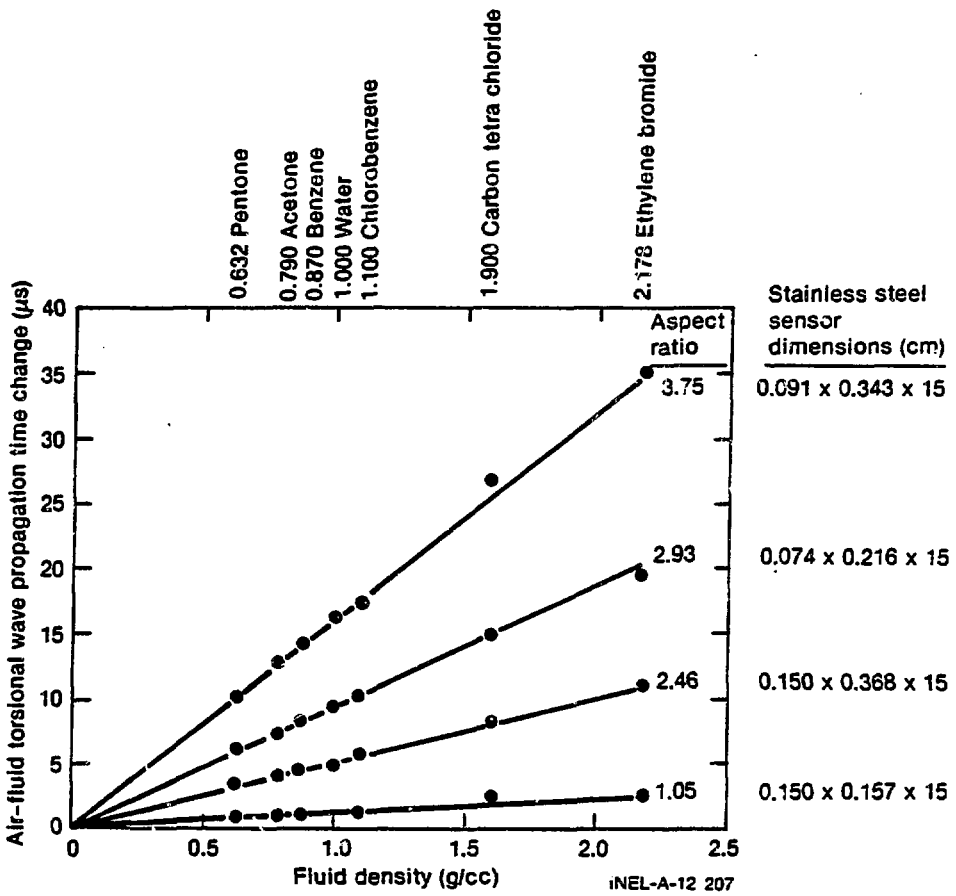

Fig. 5 Single-phase density calibration data.

TABLE I

SENSOR CHARACTERISTICS VERSUS SHAPE

Shape	Size (mm)	Aspect ratio (width/thickness)	Propagation time, t_o (s/cm)	Density Sensitivity (% of t_o)
Oval	2.28 x 6.35 x 34.92	4.16[a]	8.6	5.8
Air foil	1.52 x 6.35 x 34.92	8.32[a]	11.4	13.7
Air foil	0.99 x 3.30 x 17.78	6.50[a]	12.6	11.1
Rectangular	1.52 x 6.35 x 34.92	4.16	8.6	7.0
Rectangular	0.99 x 6.35 x 34.92	6.25	9.7	9.0
Rectangular	0.56 x 3.17 x 18.79	5.68	12.8	8.3
Rectangular	0.35 x 2.54 x 17.78	7.14	16.3	10.3

a. Average.

also checked and is listed in Table I and plotted in Figure 6. The data show that (a) the larger the aspect ratio, the longer the propagation time and (b) to have the equivalent propagation time and density sensitivity of a larger aspect ratio sensor, the sensor length must be shortened. Other shape considerations noted were:

(1) Large aspect ratios generate a dispersive wave that deteriorates in shape with distance but usually is not a problem since the sensors are too short to respond to this effect.

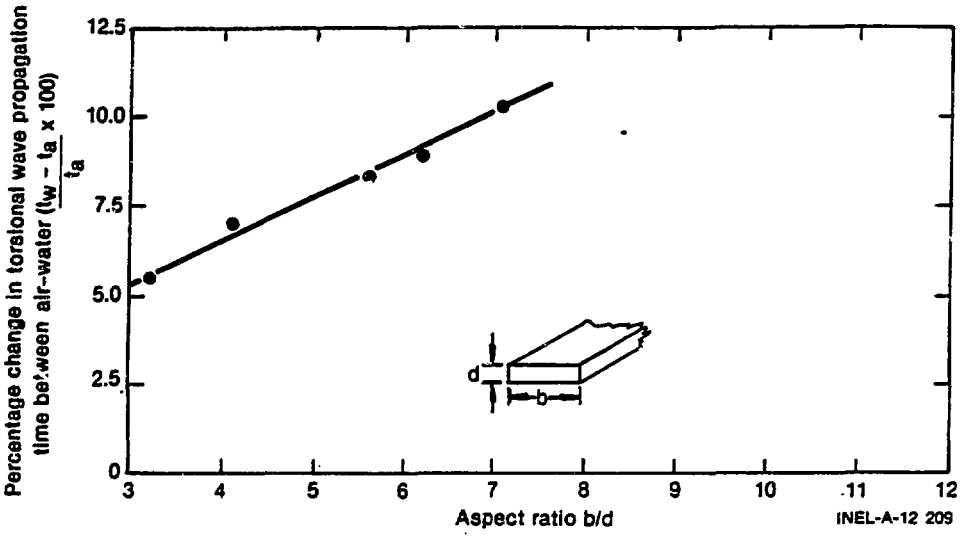

Fig. 6 Air-water density sensitivity versus sensor aspect ratio.

(2) Shapes other than rectangular do not have well behaved torsional waves and are dispersive, but in many cases do provide a density sensitivity and wave shape that can be used.

ANALYTICAL MODEL OF DENSITY SENSITIVITY

The analytical model derived subsequently relates propagation time to media density at the sensor surface and sensor temperature. From this model, equations are derived for calculating density in terms of total propagation time, changes in propagation times, sensor temperature, and predetermined constants.

The torsion wave propagation velocity can be expressed as

$$c = \frac{d}{t} = \frac{Ka}{J}\left(\frac{G}{\rho_g}\right)^{1/2}. \qquad (1)$$

To express this equation in terms of propagation time, density, and temperature, the modulus of elasticity, G, and the moment of

inertia, J, are expressed as functional dependence $G \sim K_2 - T$ and $J \sim \Delta\rho + \rho e$, respectively, where T is the sensor bar temperature, $\Delta\rho$ is the change in the density of the media surrounding the sensor bar, and ρe is the virtual density of the sensor under dry conditions. The length of the propagation path, d, the aspect ratio of the bar, Ka, and the density of the sensor bar, ρ_g, are essentially constant for the densities and temperatures of concern and can be included in one empirical constant, K_1. With this information Equation (1) can be written as

$$\frac{1}{t} = \frac{K_1}{\Delta\rho + \rho e} (K_2 - T)^{1/2} \tag{2}$$

or in terms of the density of the two-phase mixture the mathematical model as

$$\Delta\rho = K_1 \, t \, (K_2 - T)^{1/2} - \rho e. \tag{3}$$

In terms of dry initial conditions, propagation time, and temperature, the dry sensor virtual density where $\Delta\rho = 0$ can be defined as

$$\rho_e = K_1 \, t_o \, (K_2 - T_o)^{1/2} \, . \tag{4}$$

Now, the density of the media surrounding the sensor can be written as

$$\Delta\rho = K_1 \left[(K_2 - T)^{1/2} \, t - (K_2 - T_o)^{1/2} t_o\right] . \tag{5}$$

For the oven environment where $\Delta\rho = o$, the normalized propagation time dependence on temperature can be expressed as

$$\frac{t}{t_o} = \frac{t_o + \Delta t_T}{t_o} = \frac{(K_2 - T_o)^{1/2}}{(K_2 - T)^{1/2}} \, . \tag{6}$$

Substitution of Equation (6) into Equation (5) allows the density to be expressed in terms of the measured changes in propagation time:

$$\Delta\rho = \frac{K_3 t_o}{t_o + \Delta t_T} (\Delta t - \Delta t_T) \qquad (7)$$

where Δt_T is the change in propagation time from initial conditions K_2 taken from dry oven test at the same temperature, T, as the sensor when the density is being calculated. The change in propagation time due to temperature (Δt_T) is subtracted from the combined change in density and temperature propagation time from initial conditions. Equation (7) provides the density measurement in terms of initial conditions, total propagation time, changes in propagation time, and sensor temperature. A simple analysis of this equation is to note density propagation time changes are the difference of dry temperature changes and wet density and temperature changes taken from initial conditions (Δt-Δt_T); as temperature changes the constant of $(\frac{K_3 t_o}{t_o + \Delta t_T})$, between time and density, the sensitivity changes effectively the same as changing the sensor length.

Equation (7) is for torsional waves and may not agree with empirical data from sensors with another mode of propagation mixed with the torsional mode.

TEMPERATURE SENSITIVITY

The ultrasonic propagation time in the sensor is a function of the modulus of elasticity and density of the sensor material as shown in Equation (1) of the analytical model. The modulus of elasticity propagation time temperature sensitivity can be a problem under transient temperature conditions and can be reduced by selection of a material with a small change in the modulus of elasticity versus temperature. For binary nickel-iron alloys the temperature coefficient of elasticity is 0 at about 27 and 44% nickel. The addition of titanium gives a precipitation-hardened alloy in which the effective nickel content can be controlled by critical heat treatment. The further addition of chromium makes the heat treatment less critical. Such materials are Elinvar (Incoloy 902) and Incoloy 903 with chemical composition as

listed in Table II. Temperature sensitivity tests in the oven up to 350°C show the improvement over stainless steel to be a factor of ten, as shown in Figure 7.

TABLE II

ELINVAR AND INCOLOY 903 CHEMICAL COMPOSITION

Materials	Elinvar [Incoloy 902 (%)]	Incoloy 903 (%)
Nickel	45	38
Chromium	5	--
Titanium	2.75	1.4
Carbon	0.04	--
Aluminum	0.30	0.40
Silicon	0.50	--
Cobalt	0.35	15
Columbium	--	3
Iron	Balance	Balance

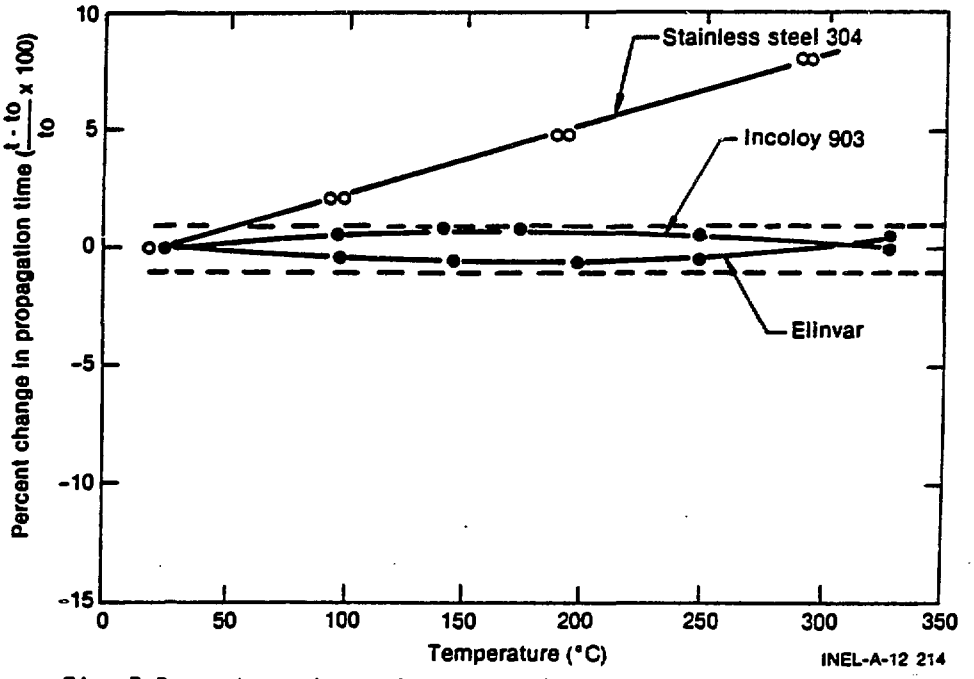

Fig. 7 Percentage charge in propagation time versus temperature.

PERFORMANCE IN TWO-PHASE FLOW

Performance of the ultrasonic density detector is as expected for an intrusive two-phase flow density measurement. The average density is the sum of the gas density and water density, but the density of the water is disturbed at the sensor surface by velocity dependent boundary layer conditions. Performance is acceptable when sensor design and limited fluid or gas velocities minimize boundary layer conditions. Air-water data and steam-water transient data for specific designs are presented with comments about accuracy versus flow regime.

Air-water performance was tested in four flow regimes with a 6.40- x 0.56-mm rectangular sensor. The LUD output was compared with that from a gamma densitometer output over approximately the same

vertical path. The data for each flow regime are shown in Figures 8 through 11. By visual observation, through a transparent test section, two basic flow effects were identified: (a) bubble masking on the sensor surface in the flow separation recirculation zones and (b) mist flow droplet holdup in the recirculation zone on the sensor surface.

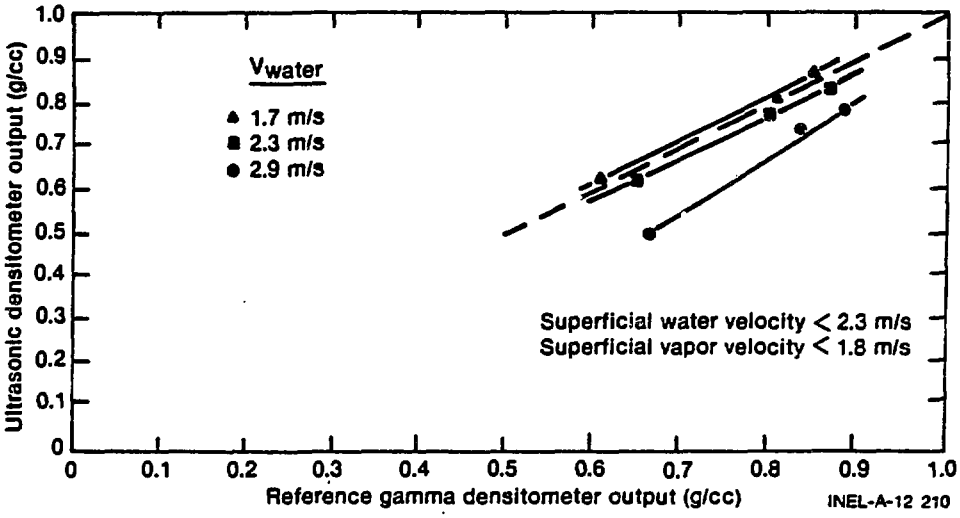

Fig. 8 Air-water test points versus flow regime.

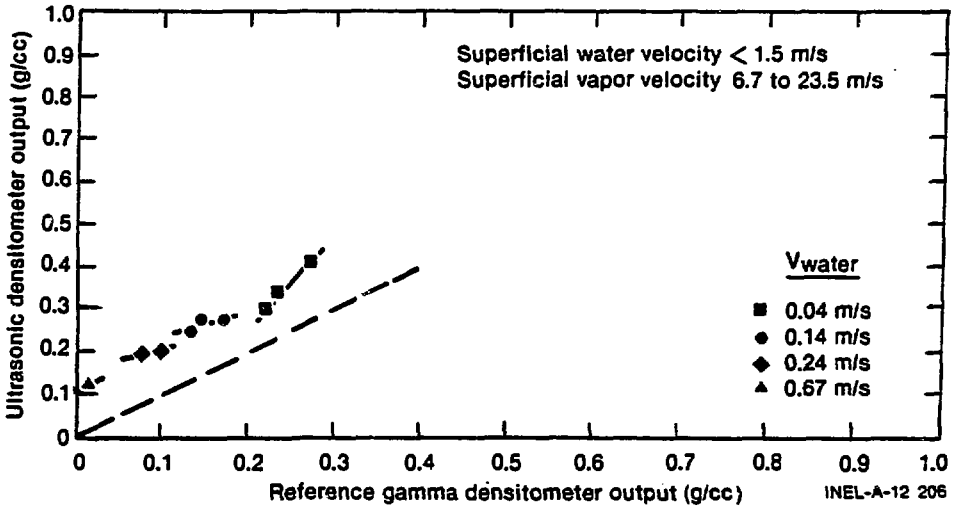

Fig. 9 Ultrasonic versus gamma densitometer stratified and plug flow data.

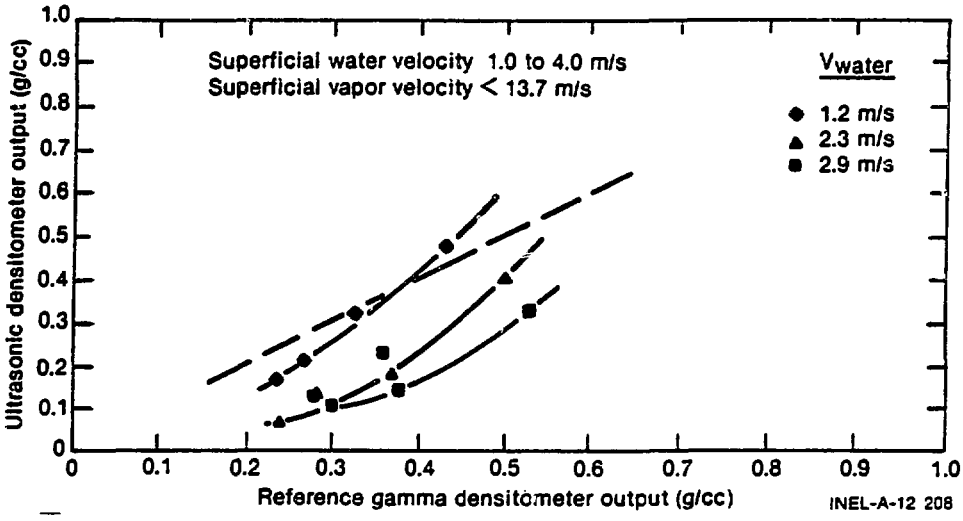

Fig. 10 Ultrasonic versus gamma densitometer mist flow data.

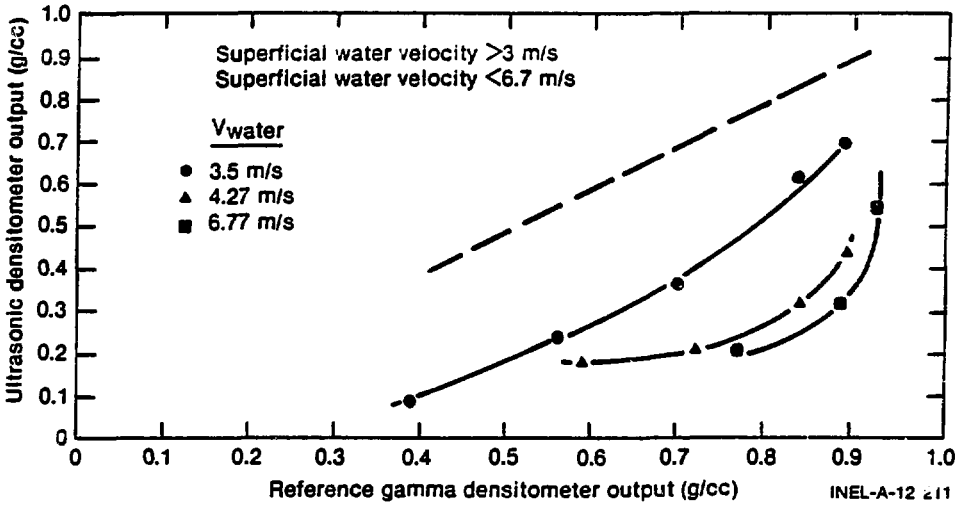

Fig. 11 Ultrasonic versus gamma densitometer slug flow data.

To increase the understanding of sensor performance in different flow regimes, the test data numbers are plotted on a 1.72-MPa steam-water flow regime map by Mandhane[9] for horizontal flow (Figure 12). Dotted lines are placed on the map to outline the sensor air-water performance in terms of flow regime. The flow effects, bubble masking, and water holdup in the flow separation recirculation zones

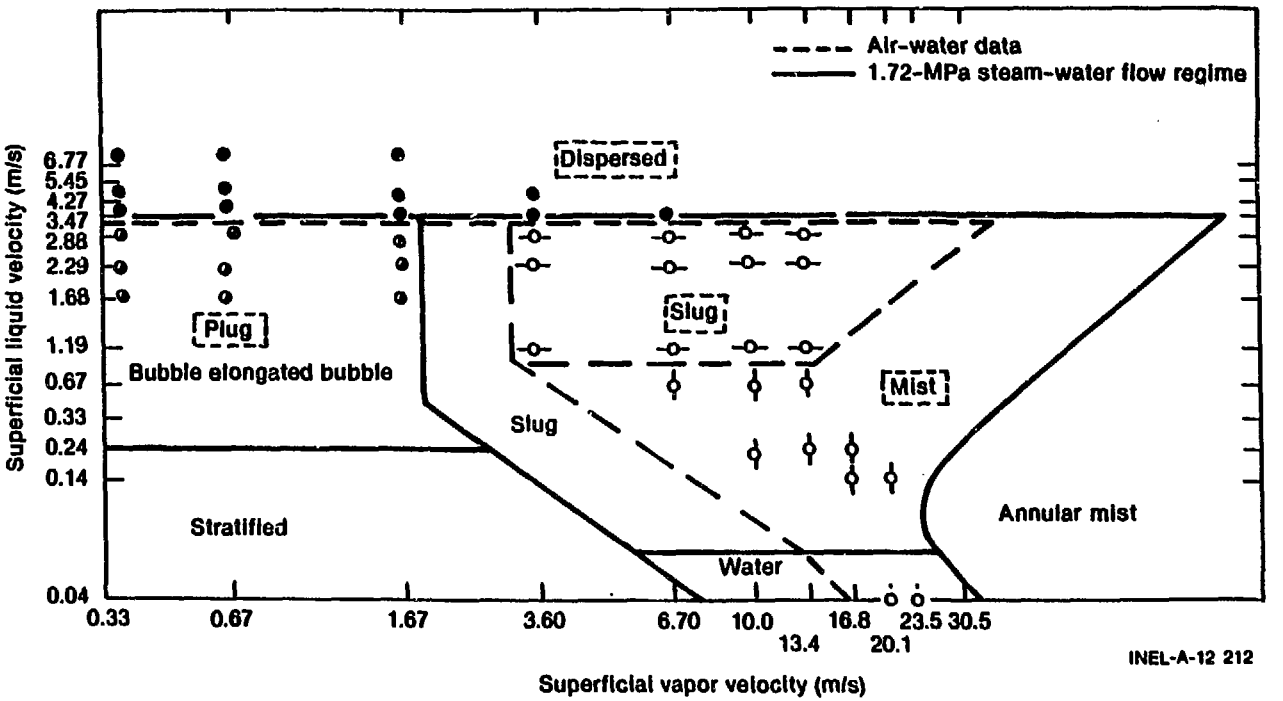

Fig. 12 Ultrasonic versus gamma densitometer dispersed bubbly flow data.

that comprise the detector performance can be identified with data points that are in groups similar to the characterized steam-water flow regimes.

Correlation between the gamma and the ultrasonic densitometer varied from excellent to poor depending on the flow regime (see Table III). The flow regime represents a combination of superficial water and superficial vapor velocities that affect the sensor performance. The results are analyzed best when stratified and plug, mist, slug and elongated bubble, and dispersed flows are considered separately. These flow types are discussed in the following sections.

TABLE III

AIR-WATER FLOW DATA VERSUS FLOW REGIME DATA

Superficial Water Velocity (m/s)	Superficial Gas Velocity (m/s)	Flow Regime	Agreement in Data
2.3	1.8	Stratified and plug	Excellent
1.5	6.7 to 23.5	Mist	Good
1.0 to 2.9	3.0 to 14.0	Slug and elongated bubble	Partial
3.0	10.0	Dispersed and bubbly	Poor

STRATIFIED AND PLUG FLOW

In stratified and plug flow, the agreement between the gamma densitometer and the LUD was excellent (Figure 8). The agreement is due to no flow separation at the sensor as a result of the lower flow rates (less that 2.9 m/s liquid and less than 1.8 m/s gas). As water flow increases beyond 2.3 m/s and is perpendicular to the front edge of the rectangular sensor, a recirculation zone builds up on the edges and is dominated by the gas bubbles. This effect masks part of the probe sensitivity.

MIST FLOW

The agreement between the gamma densitometer and the LUD was good in mist flow. In mist flow (less than < 1.5 m water and 6.7 to 23.5 m/s gas), the probe is sensing the presence of water droplets. As the droplets strike the front edge of the probe, they are captured in the recirculation zone along the side surfaces. This makes the density appear to be higher than it really is. Figure 9 shows the average values of these data points.

SLUG FLOW

In slug flow, the gamma densitometer and the LUD are in partial agreement. In slug flow (1 to 2.9 m/s water and 3 to 14 m/s air), the velocity of the water is high enough to generate a recirculation zone on the side of the probe. The amount of probe area masked by gas captured in the zone varies with superficial water velocity, void gradient, and the height of the water slugs. Average data values are plotted in Figure 10. Masking of the sensor by gas in the recirculation zone can only exist for the portion of the sensor in bubbly flow and is not stable because of the variations in the flow pattern over the length of the sensor.

DISPERSED BUBBLY FLOW

Dispersed bubbly flow produces poor agreement between the gamma densitometer and the LUD. In dispersed bubbly flow (greater than 3 m/s water and less than 10 m/s gas), a large stable bubble mask is formed on the surface of the sensor in the recirculation zone. This bubble mask prevents the sensor from seeing the true void fraction. Data are plotted in Figure 11.

Further testing in bubbly dispersed flow resulted in the following conclusions:

(1) A sensor design that minimizes flow separation cannot capture vapor in the recirculation zone on the density sensitive surface of the sensor and therefore, minimizes flow effects.

(2) A smaller density sensitive surface (small sensors) reduces flow effects.

(3) Flow separation is reduced by: (a) air foil shapes, (b) all the density sensitive area facing into the flow, and (c) smooth polished surfaces.

(4) The angle of attack of the flow on sensors is critical to increasing or decreasing flow separation.

(5) A sensor with density sensitivity only on one side has the minimum dependence of performance on the angle of flow attack when oriented with the sensitive surface perpendicular to the flow.

The transient steam-water flow test in a blowdown facility was conducted to define the performance of the 2.28- x 6.35- x 34.92-mm oval sensor in a PWR environment by comparing the output to that of a gamma densitometer with a single beam over approximately the same vertical path. The initial conditions for the blowdown facility were 5.37 MPa and 257^{o}C. The ultrasonic density detector output was corrected for temperature sensitivity and compared to the gamma densitometer on the same graph shown in Figure 13. The first 40 s show good agreement between the two but a deviation as large as 10% of range occurs during the next 50 s. This higher density deviation from the gamma densitometer is attributed to water holdup in the recirculation zone at the surface of the sensor bar as experienced in the air-water mist data. The good agreement for the first 40 s of blowdown is attributed to the velocity of the steam-water mixture being small enough that vapor bubble masking of the sensor surface was not a problem as seen in the air-water tests.

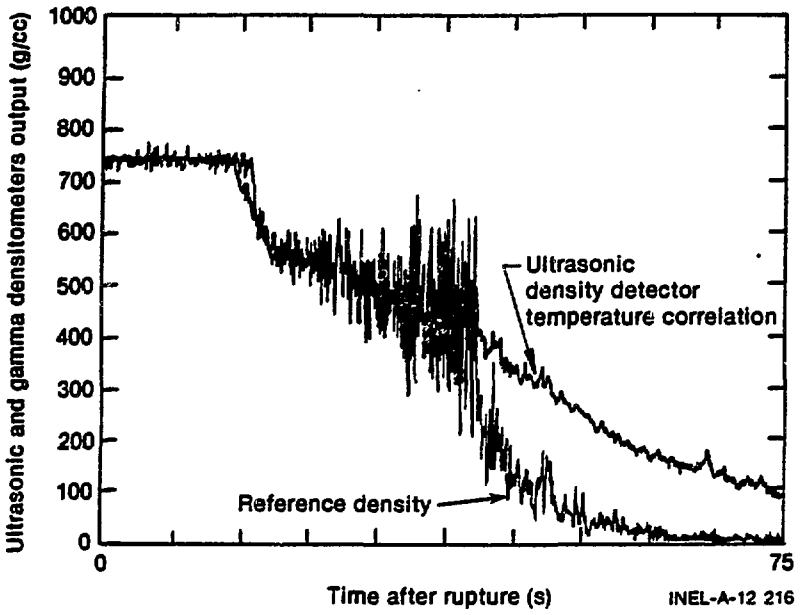

Fig. 13 Comparison of LUD and gamma densitometer transient steam-water data.

CONCLUSIONS

The ultrasonic densitometer sensor performs well for many flow applications. In comparison, the ultrasonic and gamma densitometer measure the same media properties but are different in that the former yields an intrusive measurement and the latter yields a nonintrusive measurement. The ultrasonic intrusive measurement has flow effects that alter the density at the sensor surface. The air-water flow effects in a 63.5-mm-diameter horizontal pipe are significant for 1.6- x 6.3-mm sensor bar for superficial water velocities greater than 3.0 m/s. If the application is to measure the two-phase density in a pipe, the shape of the sensor should be made hydrodynamic to minimize these effects. For reactor vessel applications with vertical free-field multidirectional flow for superficial water and vapor velocity less than 3.0 m/s, the flow regime will be mostly slug and froth. For this case, the 1.6- x 6.3-mm rectangular sensor will perform well as shown by the good correlation with the gamma densitometer in the air-water tests.

Survivability of the ultrasonic density detector is excellent with the all stainless steel interfaces to the corrosive PWR environment.

Design of the sensor and transducer may have configuration possibilities, some of which could be applied to measurements between fuel rods in a nuclear reactor core.

REFERENCES

1. A. E. Arave, An Ultrasonic Void Fraction Detector Using Compressional Stress Waves in a Wire Helix, IN-1441 (October 1970).

2. A. E. Arave, Ultrasonic Liquid Level Detector Using Surface Wave Attenuation in a Tube, ANCR-1047 (January 1972).

3. A. E. Arave, An Ultrasonic Liquid Level Detector Using Shear Wave Attenuation in a Bar, IN-1442 (November 1970).

4. L. C. Lynworth, "Slow Torsional Wave Sensors," Proceedings of IEEE Ultrasonic Symposium, 1977.

5. W. Shurtliff, A. Arave, and E. Fickas, "Ultrasonic Void Fraction Detector for In-Core Dynamic Measurements," Proceedings of the 24th International Instrumentation Symposium, Vol. 24, 1978.

6. A. E. Arave, E. Fickas, "Progress Report on LOFT Ultrasonic Density Detector for Fuel Inlet Blowdown Measurements," Proceedings of NUREG Two-Phase Flow Instrumentation Review Group Meeting, March 1978.

7. A. E. Arave, F. E. Panisko, High Temperature Ultrasonic Thermometer In-Reactor Fuel Rod Centerline Temperature Test Results, ANCR-1091 (October 1972).

8. A. E. Arave, Herry Buchenauer, Use of Tungsten - 2% Thoria Ultrasonic Transmission Line and Sensor to Improve the Performance of High-Temperature Ultrasonic Thermometry, TREE-NUREG-1021 (November 1976).

9. Mandhane et al, Instrument Journal Multiphase Flow, (1974) pp 537-553.

ACKNOWLEDGMENTS

Recognition must be given to Larry Lynnworth of Panametrics, Inc., for identification of the sensor technique, Grant Cheevers and Mike Dacus for mechanical prototype designs, Al Donaldson for materials suggestions, Dave Collins and Stan Englert for prototype fabrication, and Charles Jeffery for test engineering support.